

AD-A096 472

VARIAN ASSOCIATES INC PALO ALTO CA

F/G 20/7

FUNDAMENTAL RESEARCH OF MOLECULAR BEAM EPITAXY FOR DEVICE APPLI--ETC(U)

NOV 80 Y 6 CHAI

F49620-80-C-0011

UNCLASSIFIED

AFOSR-TR-81-0157

NL

1 CR 1
AD A
96472



END
DATE
FILMED
4 -8
DTIC

AFOSR-TR- 81 - C 1 5 7

LEVEL II

12

FUNDAMENTAL RESEARCH OF MOLECULAR BEAM EPITAXY FOR DEVICE APPLICATIONS

FINAL REPORT

November 1980

DTIC
S
MAR 17
E

Sponsored by:

Air Force Office of Scientific Research
Bolling AFB, Washington DC 20332

Contract: F49620-80-C-0011

Produced by:

Y. G. Chai

Varian Associates, Inc.
611 Hansen Way
Palo Alto, CA 94303

AD A 096 472

DEC FILE COPY

81 3 16 002

Approved for release

UNCLASSIFIED

SECURITY CLASSIFICATION OF THIS PAGE (When Data Entered)

19 REPORT DOCUMENTATION PAGE		READ INSTRUCTIONS BEFORE COMPLETING FORM	
1. REPORT NUMBER	2. GOVT ACCESSION NO.	3. RECIPIENT'S CATALOG NUMBER	
(18) AFOSR/TR-81-0157	AD-A096472		
4. TITLE (and Subtitle)	5. TYPE OF REPORT & PERIOD COVERED		
(6) FUNDAMENTAL RESEARCH OF MOLECULAR BEAM EPITAXY FOR DEVICE APPLICATIONS	(7) Final rept. 1 Oct 79 - 30 Sept 80		
7. AUTHOR(s)	8. CONTRACT OR GRANT NUMBER		
(10) Y. G. Chai	(15) F49620-82-C-0011		
9. PERFORMING ORGANIZATION NAME AND ADDRESS	10. PROGRAM ELEMENT PROJECT TASK AREA & WORK UNIT NUMBERS		
Varian Associates, Inc. 611 Hansen Way Palo Alto, CA 94303	(17) C1 230501		
11. CONTROLLING OFFICE NAME AND ADDRESS	12. REPORT DATE		
Director of Electronic & Solid State Sciences Air Force Office of Scientific Research Bolling AFB, Washington, DC 20332	(11) November 1980		
13. DISTRIBUTION STATEMENT (of this Report)	14. NUMBER OF PAGES		
(12) 43	43		
15. DISTRIBUTION STATEMENT (of the abstract entered in Block 20, if different from Report)	16. SECURITY CLASSIFICATION (if known)		
	Unclassified		
17. DISTRIBUTION STATEMENT (of the abstract entered in Block 20, if different from Report)	18. DECLASSIFICATION SCHEDULE		
19. KEY WORDS (Continue on reverse side if necessary and identify by block number)			
Molecular Beam Epitaxy (MBE)		Si doping	
GaAs		accelerated growth rate	
SnTe doping			
20. ABSTRACT (Continue on reverse side if necessary and identify by block number)			
Characteristics of SnTe, Si, and Be were investigated as dopants in MBE of GaAs. SnTe exhibited substantially sharper doping profiles and lower surface segregations than elemental Sn. It appears that SnTe molecules incorporate mostly as Sn and Te pairs instead of independent Sn and Te atoms, and that this incorporation mechanism suppresses the surface segregation. It was also found that SnTe incorporation depends on the availability of Ga vacancies. The intensities of Sn and Te in the SnTe-doped films were comparable, as expected from			

364100

UNCLASSIFIED

~~UNCLASSIFIED~~

pair incorporation. The exact nature of the pair incorporation mechanism is not understood. It does not appear that SnTe incorporates as a molecule, since in that form it would give rise to a deep donor (25 meV-30 meV), which was not found in SnTe-doped films. DLTS measurements indicate that SnTe does not introduce detectable densities of deep traps in the film.

Si was also studied in conjunction with accelerated growth rates. Si-doped films exhibited high mobilities and good photoluminescence (PL) characteristics. Lower energy peaks observed by others in liquid nitrogen temperature spectrum were not seen in our films, indicating these peaks are not inherently connected with Si doping. The accelerated growth rates did not affect the PL characteristics and only improved the liquid nitrogen mobilities.

Be doping was studied in the range from 10^{16} to $10^{19}/\text{cm}^3$. Satisfactory hole mobilities and p-n junctions were obtained, indicating adequate purity of the Be source.

5-10-16 16 19 cm³
5-10-16 19 cm³ / cc

TABLE OF CONTENTS

<u>Section</u>	<u>Page</u>
I. INTRODUCTION	1
II. EXPERIMENTAL	5
III. RESULTS AND DISCUSSION	8
A. Dopant Incorporation of SnTe in MBE GaAs	8
B. Si Doping of MBE-GaAs in Conjunction with Accelerated Growth Rates	18
C. Be Doping and Others	28
IV. CONCLUSIONS	31
REFERENCES	33
PUBLICATIONS	35

Accession For	
NTIS GRA&I	<input checked="" type="checkbox"/>
DTIC TAB	<input type="checkbox"/>
Unannounced	<input type="checkbox"/>
Justification	
By _____	
Initial _____	
Avail _____	
Avail _____	
Spec	Special
A	

AIR FORCE SYSTEMS COMMAND (AFSC)
NOTICE: This document is prepared and is
distributed in accordance with AFM 100-12 (7b).
Distribution is unlimited.
A. D. BLOOM
Technical Information Officer

I. INTRODUCTION

Recently, the molecular beam epitaxy (MBE) technique has rapidly become a practical epilayer growth technique for optoelectronic and microwave devices.^{1,2} In spite of all the advantages that MBE has, however, finding an ideal n-type dopant has been pointed out as one of the problem areas.³ Sn is currently most widely used, but its incorporation depends on its surface population,⁴ making it difficult to achieve an abrupt change in doping profile. One result of this surface segregation is that it produces a doping concentration dip when grown on n^+ substrates, resulting in high series resistance for IMPATT and mixer diodes. Another column IV amphoteric dopant, Ge, does not have the surface segregation problem but is strongly amphoteric and its doping effect is very sensitive to growth conditions. In fact, two layers of opposite polarity can be grown successively on the same wafer simply by changing the substrate temperature during growth.⁵ Si does not have segregation problems nor is it as amphoteric as Ge. High mobility and sharp doping profiles have been demonstrated by using Si.^{6,7} One problem of using Si, however, is its photoluminescence (PL) characteristic.^{8,9} At 77°K, there always was observed a peak about 1 eV below the band edge emission peak, which was associated with Ga vacancies by other workers. This peak appeared to make Si doping less attractive for optoelectronic devices.

Owing to shortcomings of these dopants, we investigated SnTe as a source of donor impurities. Both Sn and Te are known donors in GaAs, and there is a good possibility that both Sn and Te incorporate as donors in MBE-GaAs. The initial results with SnTe doping were encouraging. The Hall mobilities measured on SnTe-doped films were comparable to Sn-doped films. More importantly, a sharp doping profile was obtained using SnTe without predeposition. As an example, the doping profiles of

three MBE-grown GaAs films are shown in Fig. 1. Film (1) was grown using Sn doping at a substrate temperature of 544°C, following a Sn predeposition of 15 minutes. The film (2) was also grown using Sn, but at a substrate temperature of 581°C and with Sn predeposition time of 45 minutes. Film (3) was grown using SnTe at a substrate temperature of 581°C with no predeposition of SnTe. This result clearly shows that doping with SnTe produces sharper doping profile than doping with Sn, and that predeposition steps can be eliminated when using SnTe. This capability of obtaining a sharp doping profile makes SnTe an attractive alternative to Sn.

Prior to this contract, we had seen anomalous p-n junction behavior on SnTe/Be-doped films. Also, liquid nitrogen temperature mobilities were low (about 40,000 cm²/V-sec). Therefore, we planned extensive studies on background impurity incorporation and gettering of the undesirable impurities, believing that these were the cause of the anomalous junction behavior and low mobilities. However, with continuous use of the system, the mobilities steadily improved and we have obtained the maximum 77°K mobilities of 75,000 cm²/V-sec recently. Also, as the text will later show, the total deep trap densities are so low that it is difficult to even detect them. Therefore, some of the planned studies on background impurity incorporation were obviated. Instead, the efforts were redirected to study Si doping, which was not originally proposed.

One motivation was to cut down the growth time of some microwave devices. For example, the growth of 19-GHz IMPATT diodes takes 8-9 hours; a doubling of growth rate would cut the growth time by half. Further increase in growth rate, of course, should cut down the growth time further. In order to investigate higher growth rate effects, it was desirable to find a dopant which is least sensitive to change of growth conditions. SnTe was still under investigation at that time, but

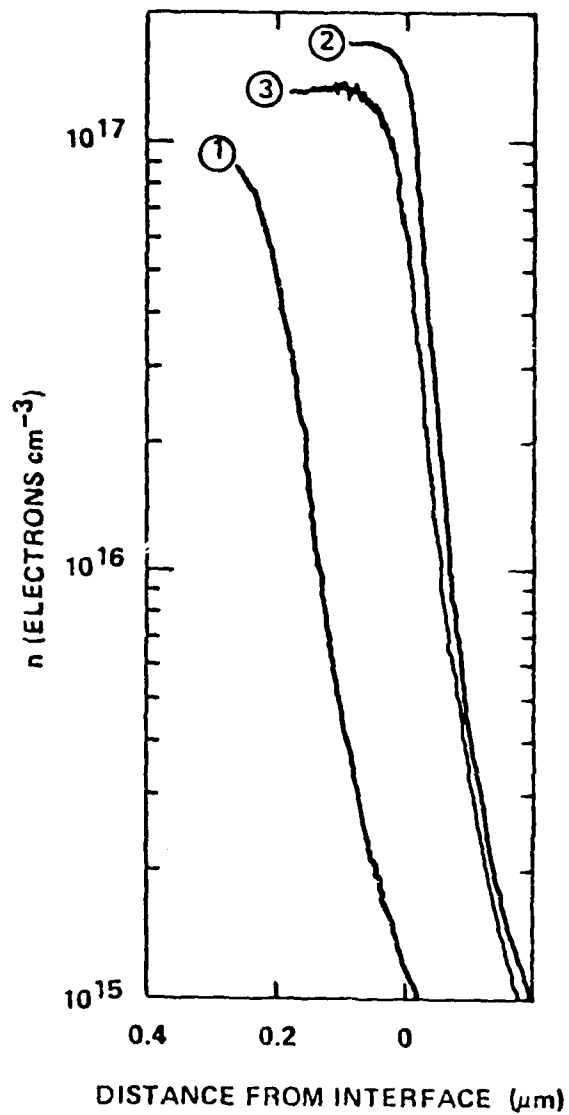


Fig. 1 Doping profiles for three different MBE GaAs films:

- (1) Sn doped, $T_{\text{sub}} = 544^{\circ}\text{C}$, 15 min. Sn predeposition.
- (2) Sn doped, $T_{\text{sub}} = 581^{\circ}\text{C}$, 45 min. Sn predeposition.
- (3) SnTe doped, $T_{\text{sub}} = 581^{\circ}\text{C}$, no dopant predeposition.

its incorporation was not well understood. Alternatives were Sn, Ge and Si. Among these, Si appeared to be least sensitive to growth conditions. It had been reported that Si incorporation rate is independent of substrate temperature from 500-600°C and is sensitive to As₄/Ga ratio change.⁹

Our initial experimental results were gratifying. Si doping was not only compatible with higher growth rate, but also did not produce the lower energy photoluminescence peak which was observed by other researchers at 77°K, indicating good electro-optical characteristic of Si-doped films. These experimental results and others are presented in this report.

II. EXPERIMENTAL

All the epitaxial growths were performed in a Varian MBE-360 molecular beam epitaxy system. The system has three chambers -- a wafer interchange-load lock chamber, interlock chamber, and growth chamber. The load-lock chamber protects the interlock chamber from exposure to the atmosphere, and the interlock chamber allows the growth chamber to see only high vacuum on the order of 10^{-10} Torr scale, so that ultrahigh vacuum conditions are readily maintained in the growth chamber. Also, the interlock chamber has a carousel which can hold four heater blocks so that a run can be made immediately after another by simply transferring out the grown wafer from the growth chamber and transferring in a new substrate which has been stored in the interlock chamber under high vacuum.

An exploded view of the growth chamber is shown in Fig. 2. The growth chamber has 8 furnaces, 8 furnace shutters, and a substrate carousel. The carousel has two substrate holders. Not shown in the figure is an ion gauge attached to the carousel which can be placed in the path of molecular beam by simply rotating the carousel. The beam flux was measured by opening and closing a furnace shutter and measuring the pressure difference using this ion gauge. The Auger analysis components are on the right side of the chamber and analytical components, reflection electron diffraction and a quadrupole mass spectrometer are on the left side of the chamber.

The molecular beam sources were standard Varian MBE furnaces containing charges of Ga (7N, Eagle-Pitcher), As (6N, Canyonlands 21st Century Corp.), SnTe (5N, Alpha-Ventron), Si (10^{13} cm⁻³ phosphorous-doped Dow Corning), and Sn. All the charges were obtained in pyrolytic boron nitride (PBN) crucibles. The substrate material was (100)-oriented, Cr-doped or Sn-doped GaAs grown at Varian by the liquid encapsulation Czochralski process; Sn-doped GaAs substrates purchased from Mitsui were

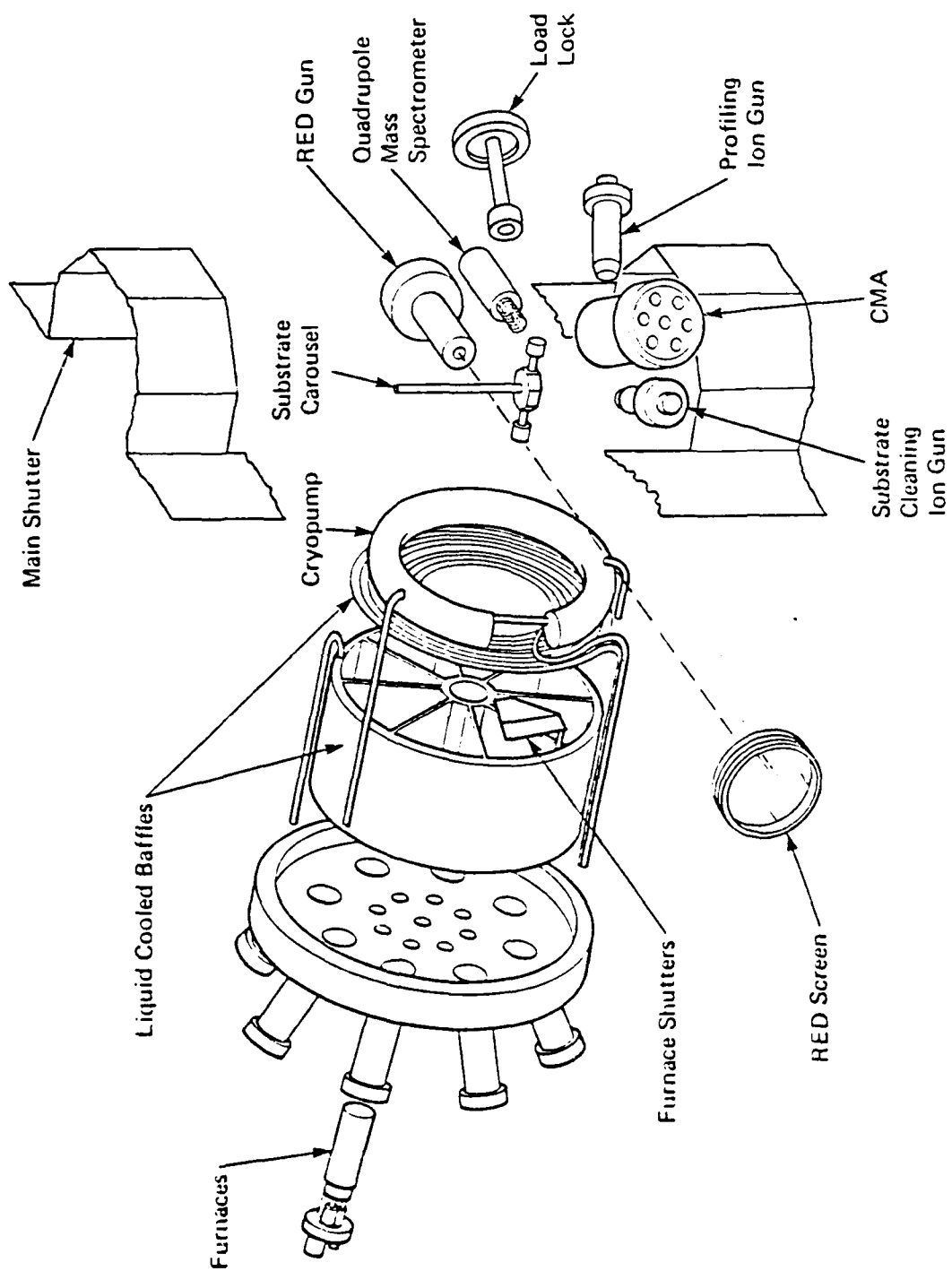


Fig. 2 Exploded view of the growth chamber in Varian MBE-360 system.

sometimes used. The substrates were chemo-mechanically polished in a standard sodium hypochlorite solution. Immediately before loading, the substrates were degreased in TCE, acetone, and methanol and etched in stagnant 4:1:1 ($\text{H}_2\text{SO}_4:\text{H}_2\text{O}_2:\text{H}_2\text{O}$) solution for one minute. Indium was used to bond the substrate to a molybdenum heater block. The substrate was heat cleaned in the growth chamber for six minutes at 611°C. When the substrate temperature reached 500°C, the As furnace shutter was opened with the substrate at the growth position to prevent the substrate surface from decomposition due to possible arsenic evaporation.

The usual growth rate used was 1 μ/h unless otherwise specified. A typical As_4 -to-Ga flux ratio, $J_{\text{As}_4}/J_{\text{Ga}}$, was 0.75 to 1.00. A typical background pressure during growth was 5×10^{-7} Torr, which mostly consisted of various arsenic species. The Hall mobilities were measured by the van der Pauw technique on 2.5-3.0-micron thick layers grown directly on Cr-doped substrates without a buffer. The magnetic field was 1.2 kilogauss. The epitaxial layer thickness determined by cleave and strain measurement was used for calculation of carrier concentration. Photoluminescence (PL) measurements were made at 77°K with a 1-W argon laser and cooled S-1 photomultiplier. For the SnTe incorporation study, Secondary Ion Mass Spectroscopy (SIMS) technique was extensively used. This service was purchased from Charles Evans & Associates, San Mateo, California.

III. RESULTS AND DISCUSSION

A. Dopant Incorporation of SnTe in MBE GaAs

When either elemental Sn or Te is used as a dopant in MBE GaAs, both lead to the surface segregation problem. The problem is more severe for Te than for Sn, Te accumulating to several monolayers at the surface. It has been reported that Te_2 actually displaces the outer layer of arsenic atoms from the As-stabilized structure to form stable surface compound Ga-Te.¹¹ This severe Te accumulation is not seen in SnTe-doped films. Figure 3 shows SIMS results on a SnTe-doped layer grown at 533°C. It should be pointed out that the difference in the ion counts for Sn and Te is due to the different sensitivity of the SIMS technique to these elements, and that their actual concentrations are about the same, as will be shown later. The small spike on the right side of the profile was probably caused by a high SnTe vapor pressure which had been built up behind the shutter and released when the shutter was opened. However, this result clearly shows that sharp doping profile steps are possible using SnTe. The total concentration of Sn and Te is about 4×10^{19} for this film.

When a higher substrate temperature is used, Sn and Te segregation begins to be noticeable. The wafer shown in Fig. 4 was grown while the substrate temperature was changed in steps from 533°C to 581°C to 612°C during growth. An undoped layer was grown at 520°C between each layer to see how the doping concentration changed after the SnTe shutter was closed. At the end, a 2.5- μm thick undoped layer was grown at 520°C and this layer was ion implanted with 2×10^{14} atoms/cm² of Sn and 1×10^{14} atoms/cm² of Te at 250 KeV. These known Sn and Te concentrations were used for the calibration of the Sn and Te concentration in SnTe-doped layers. As shown in the figure, the doping concentration of both Sn and Te decreases at a higher substrate temperatures due to re-evaporation of

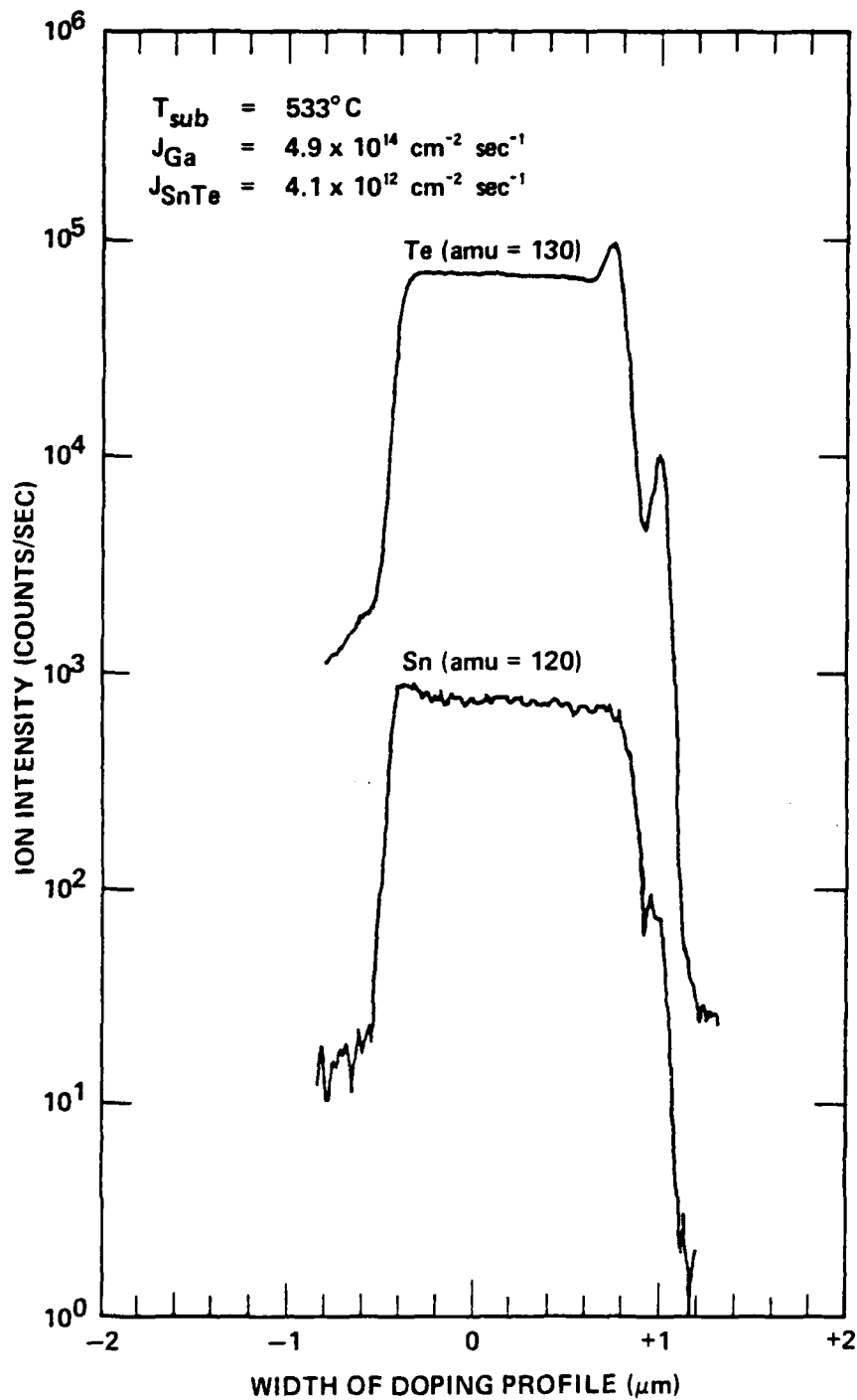


Fig. 3 Sn and Te concentration profile measured by SIMS.

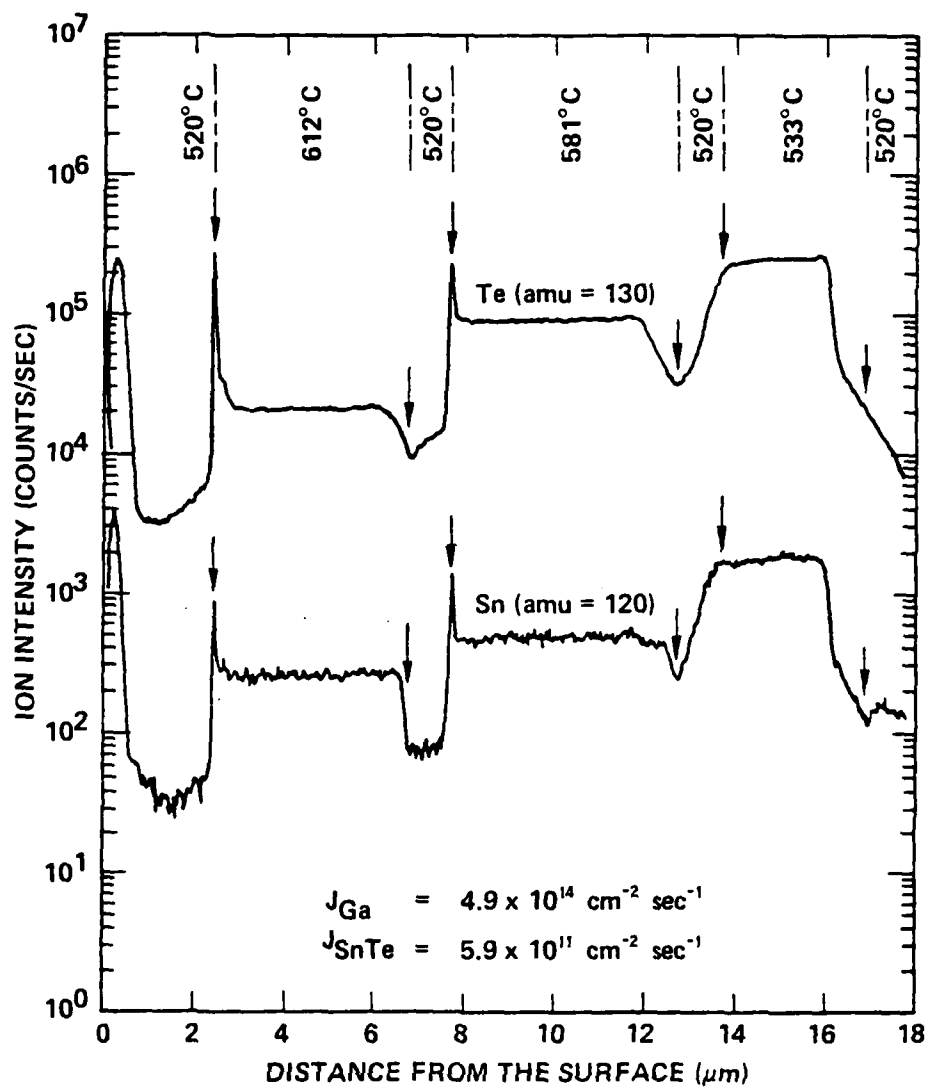


Fig. 4 Relative Sn and Te concentrations measured by SIMS as a function of depth; the substrate temperatures were changed in steps during growth of this film.

SnTe from the substrate surface. Also, the increase and decrease of the doping profile of the first layer are not sharp due to a nonuniform SIMS sputtering depth caused by surface roughness of this particular wafer. However, the doping concentration spike at the end of the layer grown at 581°C clearly shows that the Sn and Te accumulated at the surface. Even though both Sn and Te accumulate at the surface, the surface populations are not equal. The difference in the degree of accumulation for Sn and Te is clearly shown in the last layer grown at 612°C in which the amount of accumulated Te is about 4-5 times higher than that of accumulated Sn. When the total amount of accumulated Sn and Te was calculated from this figure using the known concentration of ion-implanted Sn and Te in the buffer, the total amount is only 2-4% of a monolayer, even at a high surface temperature of 612°C. Also, it may be noted that the change in Sn doping profile is more abrupt than Te, even at higher substrate temperatures.

From these results, we conclude that most of the SnTe incorporates as a Sn and Te pair, i.e., incorporation of Sn promotes incorporation of Te. If SnTe decomposes at the surface and incorporates as individual Sn and Te atomic species, the same degree of Te surface accumulation should be seen for SnTe-doped films as when elemental Te is used. This gross accumulation is not seen in our result. Furthermore, we conclude that when SnTe molecules do decompose at high substrate temperature, they decompose at Ga vacancy sites where the Sn atom readily incorporates. We base this conclusion on the lower accumulation and sharper changes in the doping profile of Sn and Te, as seen in this figure.

Even though SnTe incorporates as a pair, the amount of incorporation is determined by the availability of Ga vacancies. A wafer was grown at a constant substrate temperature of 581°C, but this time the As flux was changed in steps, thus changing the number of Ga vacancies at

the surface during growth. As seen in Fig. 5, the increase of the As flux, and thus the increase in the number of Ga vacancies, results in increase of both the Sn and Te concentration. The result clearly shows that SnTe incorporates as a Sn and Te pair (not necessarily as a SnTe molecule) and the rate of incorporation depends upon the number of Ga vacancies available.

The ratio of Te-to-Sn incorporation is shown in Fig. 6. Each wafer has 3 to 4 layers, similar to those shown in Figs. 4 and 5. The summary of growth conditions is shown in Table I. Figure 6 shows that in all cases the Te/Sn ratio is close to unity (shown as a solid line in the figure), confirming the Sn and Te pair incorporation conclusion. In the majority of cases, the amount of Te is somewhat less than the amount of Sn, and the difference becomes larger at higher substrate temperatures. This indicates that Te evaporates from the substrate surface during growth in a form other than SnTe. It appears that some of the Te accumulated at the surface evaporates as volatile Te_2 , because the Te_2 peaks were observed by a quadrupole mass spectrometer scan when the substrate temperature was raised to 633°C with the SnTe shutter closed. No observable Te_2 peaks could be found with a cold substrate and an open SnTe furnace, indicating that the source of Te_2 is not the SnTe furnace itself. We did not see evaporation of Sn from the surface.

Figure 7 shows that the net carrier concentration and total density of Sn and Te in the films as a function of the reciprocal temperature of the SnTe furnace. The former was measured by van der Pauw technique, and the latter computed from SIMS results. There are two sets of van der Pauw data, one for films grown at 533°C and the other for films grown at 581°C. The net carrier concentrations for films grown at 581°C is smaller than those for films grown at 533°C. This is probably due to re-evaporation of physisorbed SnTe molecules from the surface before incorporation. However, at both substrate temperatures, the carrier

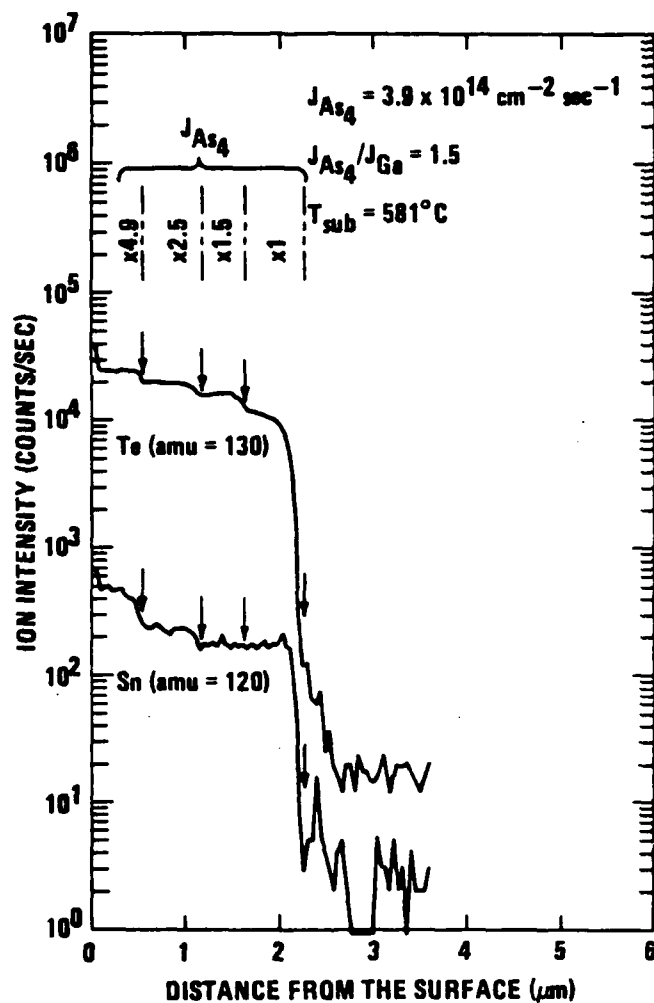


Fig. 5 Relative Sn and Te concentrations measured by SIMS as a function of depth; the As_4/Ga flux ratio was changed in steps during growth of this film.

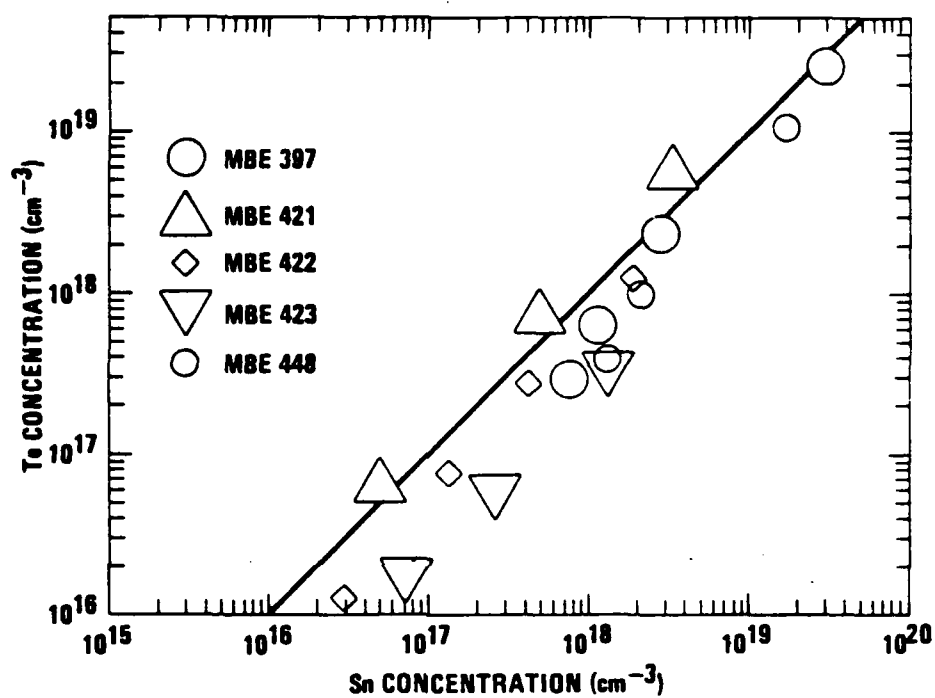


Fig. 6 Te/Sn ratio in SnTe-doped films grown under various conditions.

WATER NUMBER	VARIABLE	NUMBER OF LAYERS IN THE FILM	SUBSTRATE TEMP (°C)	SnTe FLUX (cm ⁻² sec ⁻¹)	As ₄ /Ga RATIO
397	T _{sub}	3	533 581 612	7.5 x 10 ¹¹	2.7
421	T _{SnTe}	4	533	1.1 x 10 ⁹ 1.1 x 10 ¹⁰ 7.2 x 10 ¹⁰ 1.4 x 10 ¹²	1.5
422	T _{SnTe}	4	581	SAME AS 421	1.5
423	T _{SnTe}	4	612	SAME AS 421	1.5
448	T _{sub}	3	533 581 612	5 x 10	1.1

Table 1

Summary of experimental conditions for films shown in Fig. 6.

concentration under high SnTe fluxes deviates from the straight line representing the vapor pressure curve of SnTe.¹² When the total densities of Sn and Te are plotted in the same graph, they also show similar deviations from the vapor pressure curve. Therefore, the saturation of the net carrier concentration at high doping levels cannot be explained by donor-acceptor compensation. We speculate that the Te and Sn accumulation at the surface at high SnTe furnace temperatures effectively reduces the sticking coefficient of SnTe molecules, resulting in a decrease in the Sn and Te incorporation in the growing layers.

The presence of deep donors and deep trap levels in SnTe-doped films was checked, with only negative results. The net carrier concentrations measured by the van der Pauw technique at room temperature and liquid nitrogen temperature are practically identical, indicating SnTe doping produces shallow donors. For example, the carrier concentrations measured on two samples from the same SnTe-doped wafer were $3.60 \times 10^{15} \text{ cm}^{-3}$ and $3.70 \times 10^{15} \text{ cm}^{-3}$ at room temperature, and decrease only slightly to $3.54 \times 10^{15} \text{ cm}^{-3}$ and $3.70 \times 10^{15} \text{ cm}^{-3}$ respectively at liquid nitrogen temperature.

Deep Level Transient Spectroscopy (DLTS) measurements were made on films doped with three different dopants (Si, Sn, and SnTe). The measurement technique was as follows. A 2-micron thick layer doped at $8 \times 10^{15} \text{ cm}^{-3}$ was grown on an n-type substrate. Gold dots were evaporated on the surface and the wafer was loaded into the DLTS measurement chamber. The temperature of the sample was slowly raised from liquid nitrogen temperature to 100°C overnight. As the temperature rose slowly, the Schottky-barrier capacitance was automatically measured and recorded at intervals, as a function of temperature. At the completion of the run, thermal emission rate, activation energy, trap densities, and capture cross sections were computed from these data. Table II summarizes the results. As shown, the total trap densities are less than $1 \times 10^{13} \text{ cm}^{-3}$

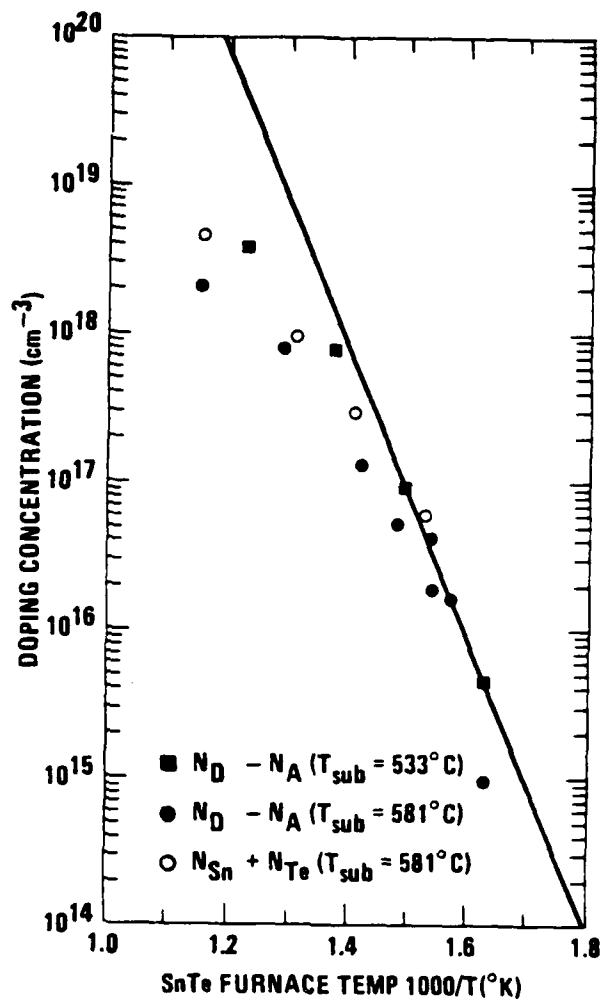


Fig. 7 Net carrier concentration and the total Sn and Te concentration in SnTe-doped films as a function of inverse temperature for the SnTe furnace.

for all the layers, indicating cleanliness of the systems we are using. It appears that the total number of deep traps in a SnTe-doped film is higher than that of a Si-doped or Sn-doped film. However, this difference in total deep trap densities can be easily attributed to the difference in growth conditions, or to the measurement itself. As shown in the table, the total trap densities are lower than 10^{13} cm^{-3} for the doping concentration shown in the table, close to the detection limit of the DLTS apparatus used. Also, the total density of traps can vary from sample to sample. For example, the DLTS results on two Si-doped films grown under the similar conditions but on different occasions show wide variations in deep trap energies and their concentration. This much is certain, however, that SnTe doping does not introduce abnormally high trap densities in the layers.

In summary, it appears that SnTe can be an attractive alternative to Sn as an n-type dopant in MBE GaAs. A sharp doping profile can be obtained with doping concentration up to $1 \times 10^{19} \text{ cm}^{-3}$ when used at a substrate temperature of 500-550°C. Sn and Te surface segregation do occur at higher substrate temperatures, but the segregation is minimal compared to elemental Sn- or Te-doped films. It appears that SnTe molecules incorporate mostly as Sn and Te pairs instead of independent Sn and Te atoms, and their incorporation depends on availability of Ga vacancies. The pair incorporation of SnTe was further evidenced by the fact that the number of Sn and Te in the SnTe-doped films is about the same. In spite of the fact that SnTe incorporates as a pair, there is no evidence that they form deep donors or that they introduce high-density deep traps in the film.

B. Si Doping of MBE-GaAs in Conjunction with Accelerated Growth Rates

One of the main features of MBE is its precise layer thickness control. It has been demonstrated that a superlattice structure,

SAMPLE #	DOPANT	$N_d - N_a / \text{cm}^3$	TRAP LEVEL (eV)	CROSS SECTION (cm^2)	TRAP DENSITY (cm^{-3})
322	Si	6×10^{15}	0.22	1.1×10^{-16}	6.8×10^{11}
			0.37	5.2×10^{-16}	5.8×10^{11}
323	Si	6.4×10^{15}	0.672	4.3×10^{-13}	8.6×10^{11}
			0.283	5.6×10^{-18}	1.5×10^{12}
			0.139	6.8×10^{-19}	1.1×10^{12}
347	SnTe	2.6×10^{16}	0.806	6.7×10^{-14}	7.1×10^{12}
			0.129	2.7×10^{-20}	1.5×10^{12}
357	Sn	2.8×10^{16}	0.626	1.6×10^{-16}	3.9×10^{12}

Table 2

DLTS data on Si-, Sn-, and Te-doped films grown by MBE.

consisting of thousands of alternating monolayers of GaAs and AlAs, can be grown by MBE.¹³ Naturally, MBE has been successful for devices that require growth of thin layers in the structure, such as lasers, mixers, IMPATT diodes, and low-noise FETs. Presently, one micron per hour (1 μ /h) is a typical MBE growth rate for GaAs. However, if higher growth rates can be employed without sacrificing device performance and yield, MBE may become an economical production process for optoelectronic and microwave devices.

In order to investigate higher growth rate effects, it is desirable to find a dopant which is not sensitive to the change of growth conditions. We chose Si because its characteristics were relatively well documented and appeared least sensitive to growth conditions. One concern was that the relatively high operating temperature required for the Si furnace ($>1200^{\circ}\text{C}$) may outgas undesirable impurities from the heating element, resulting in contamination of the growing layer. During the course of the work, however, we found that not only was this concern groundless, but also that Si is a very useful n-type dopant in MBE GaAs.

Figure 8 shows the measured carrier concentration as a function of reciprocal temperature of the Si furnace. The solid line in the figure represents the vapor pressure of Si versus $1/T$ ¹⁴ with the position of the ordinate scale adjusted to coincide with the experimental data points. The experimental points were obtained on films grown at 1 μ /h. The fact that the slope of the vapor pressure curve agrees well with the experimental points suggests that the Si doping level is proportional to the Si arrival rate over the concentration range studied. This unit sticking coefficient of Si made it easy to obtain the desired doping concentration and to determine the furnace temperature for a doping concentration needed at various growth rates.

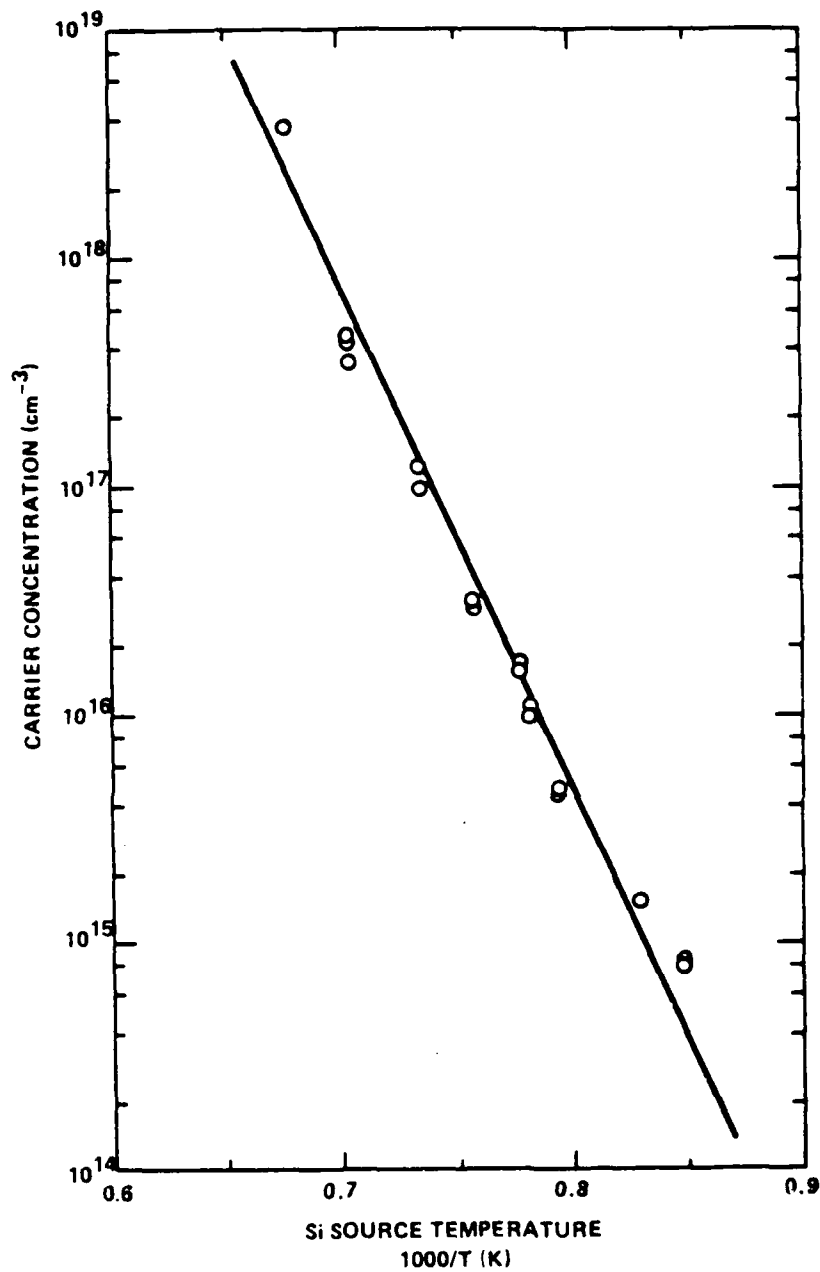


Fig. 3 Carrier concentration of Si-doped films measured by the van der Pauw technique as a function of reciprocal temperature of the Si furnace.

Hall mobilities of Si-doped films are shown in Fig. 9 as a function of doping concentration. All the films were grown at 1.0 μ /h. The results compare favorably with those reported in the literature for MBE GaAs. The highest room-temperature mobility was 8,839 $\text{cm}^2/\text{V-sec}$ at $3.6 \times 10^{15} \text{cm}^{-3}$, and the highest 77°K mobility was 60,036 $\text{cm}^2/\text{V-sec}$ at $1.2 \times 10^{15} \text{cm}^{-3}$.

Demonstrating high Hall mobilities for Si-doped films, we increased the growth rate and measured Hall mobilities on these films. The films were doped at 10^{15} - 10^{16}cm^{-3} , so that possible change in mobilities could be seen more easily. Since many different growth rates were tried, most are grouped together and presented in Fig. 10. As shown in the figure, there is about 50% spread in mobility at a given carrier concentration. A similar spread is observed even for films grown at the same rate of 1 μ /h. This variation is probably a result of compounding measurement errors and differences in substrate quality. These results show that the mobilities at higher growth rates are comparable to or higher than those at 1 μ /h. The highest 77°K mobility achieved was 75,085 $\text{cm}^2/\text{V-sec}$ at $2.2 \times 10^{15} \text{cm}^{-3}$ for a layer grown at 1.8 μ /h.

The accelerated growth rate did not produce any significant changes in the 77°K PL spectra in Si-doped films. Spectra for wafers grown at 1 μ /h and 5 μ /h are shown in Figs. 11(a) and (b). The donor-to-valence band transition at 1.507 eV dominates in both spectra. The donor-to-acceptor transition at 1.477 eV is also observed. However, the peaks observed by others in Si-doped MBE GaAs at 1.44 eV⁸ or about 0.1 eV⁹ below the edge transmission peak are very weak or absent. These peaks have been associated with an impurity-Ga vacancy complex. We therefore reasoned that small As_4/Ga ratio used for the growth of Fig. 11(a) and (b) wafers would have decreased the number of Ga vacancies. In order to check this hypothesis, a third wafer was grown with an As_4 flux five times higher than normal. PL from this wafer is shown in Fig. 11(c).

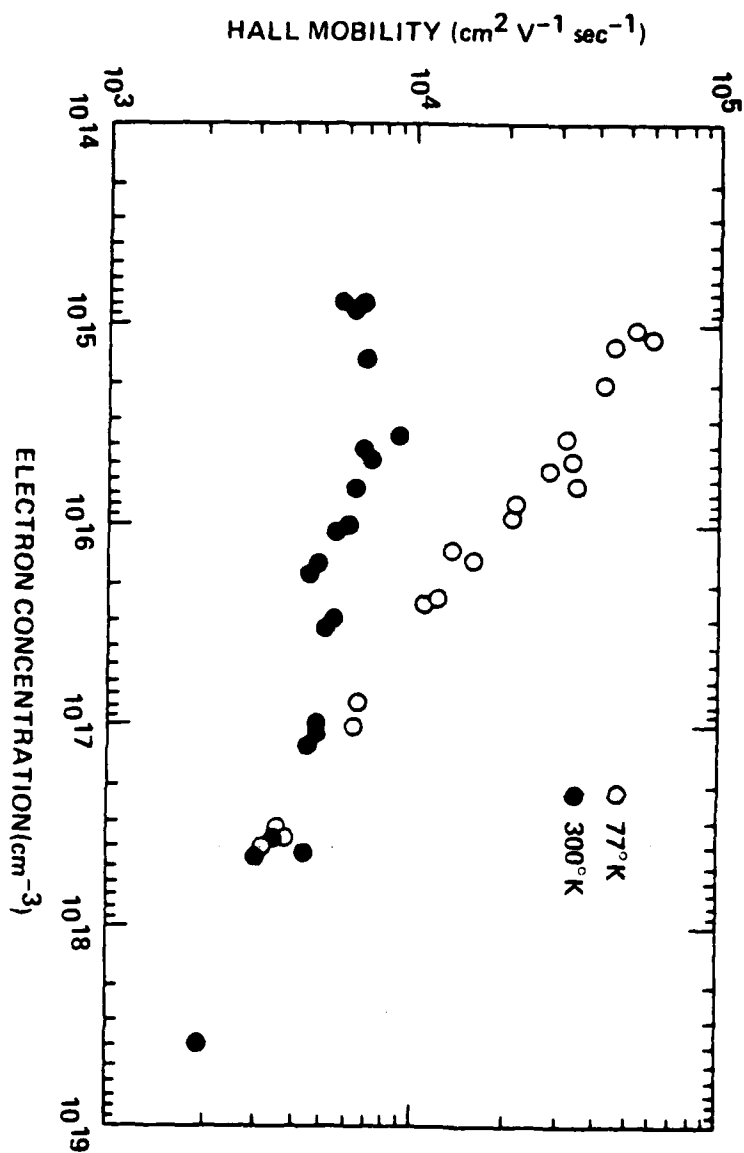


Fig. 9 Room temperature and 77°K Hall mobilities for Si-doped films grown at 1 μ /h.

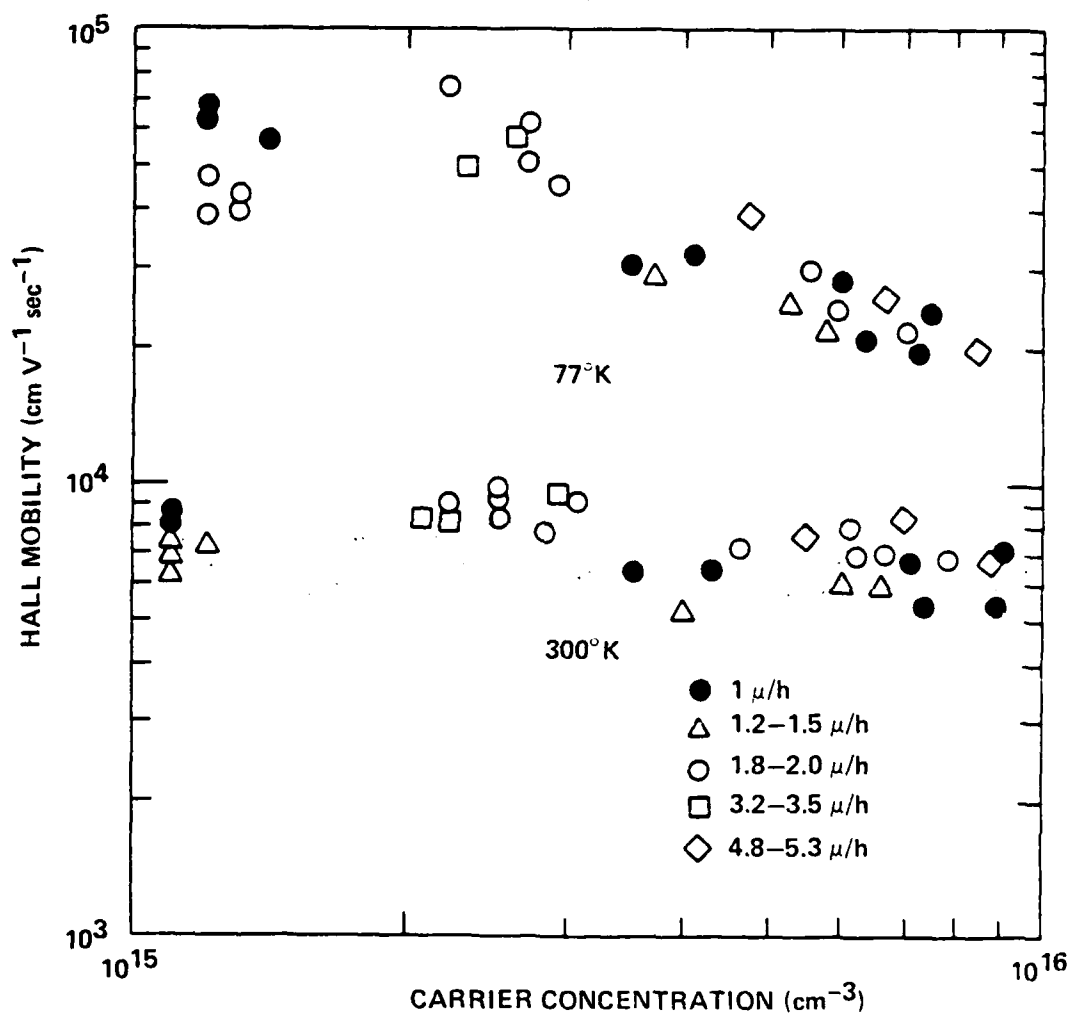


Fig. 10 Room temperature and 77°K Hall mobilities of films grown at 1-5 μ/h growth rates.

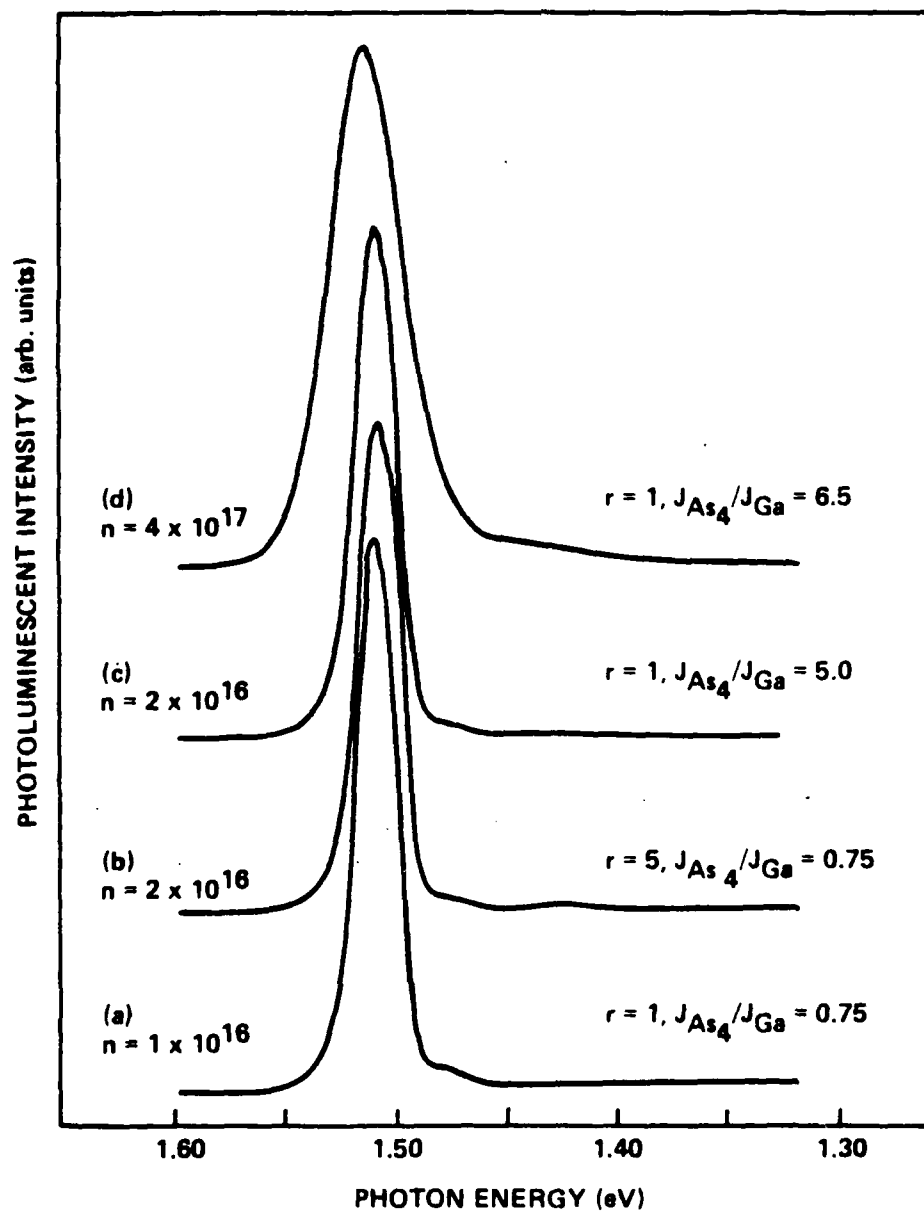


Fig. 11 PL spectrum for films grown under different conditions:

- (a) normal conditions
- (b) five times higher rate
- (c) normal growth rate but with a six times higher As_4/Ga ratio
- (d) highly doped GaAs grown with eight times higher As_4/Ga ratio

Note: r designates the growth rate.

Again, the lower energy peak is small. Finally, a highly-doped ($4 \times 10^{17} \text{ cm}^{-3}$) film was grown under very high As_4 flux density. As shown in Fig. 11(d), there is no significant increase in the lower energy peak. It is clear from these results that the lower energy peak is neither inherently connected with Si doping nor directly associated with availability of Ga vacancies as believed before, but may be associated with general cleanliness of the growth system or substrate qualities.

Low-temperature photoluminescence studies were also carried out on layers grown at $1 \mu/\text{h}$. As shown in Fig. 12, no deep levels were found in this figure either. Shallow levels were shown here were identified as due to carbon and germanium acceptors, and we see only a small peak at photon energy corresponding to the Si acceptor. The germanium peak is observable in almost all MBE-grown GaAs, including those grown by other researchers. The origin is not known. The carbon peak was always observed, but intensities were different from wafer to wafer, indicating carbon concentration depends on hydrocarbon concentration in the background gases.

In summary, Si-doped films exhibit high mobilities and good PL characteristics. Si-doped films grown at higher growth rates showed comparable or improved 77°K mobilities. The higher growth rate did not affect the PL characteristic, as shown. Most importantly, lower energy peaks observed by others in 77°K PL spectrum were not seen in our films, indicating these peaks are neither inherently connected with Si doping, nor with its capability of producing high mobilities. Good PL characteristics should make Si the most practical dopant in microwave and optoelectronic device applications, especially when higher growth rates are employed.

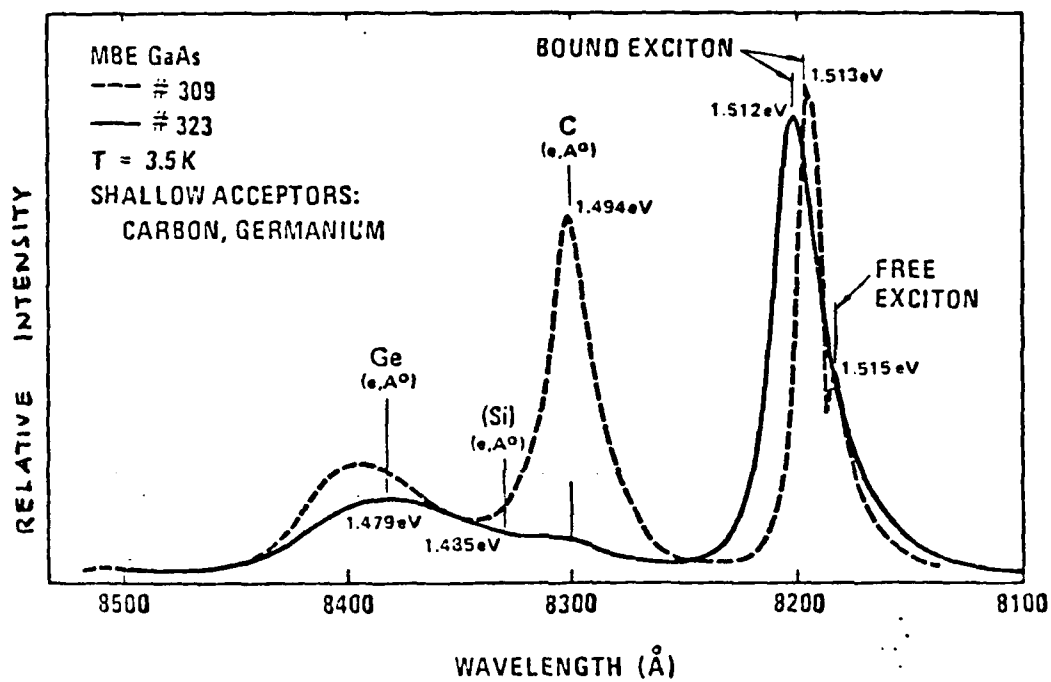


Fig. 12 Photoluminescence spectra of Si-doped MBE GaAs.

C. Be Doping and Others

(i) Be-Doped GaAs

Early studies of Be incorporation involved the growth of MBE GaAs:Be on n-GaAs layers that had been grown by vapor-phase epitaxy. Anomalous p-n junction behavior was observed, consistent with a wide compensated region at the junction. It turned out that the anomalous behavior was due neither to the MBE process itself nor to the doping characteristic of SnTe, nor is it due to low purity of the Be source (3N), commercially available.

As a means of evaluating different Be sources, Be-doped layers grown separately on Cr-doped substrates were fabricated into van der Pauw samples and mobilities measured at 77°K and 300°K. The results are displayed in Fig. 13. As can be seen, the mobilities are comparable with the best reported in the literature, indicating satisfactory purity of the Be sources. The highest mobilities were obtained with Be (4N) from Varlacoid, Co., Elizabeth, New Jersey. Also, excellent junction characteristics were obtained by continuous growth of n-p junctions in the MBE equipment using SnTe as the n-dopant, followed by the Be-doped layer. It appears, therefore, that the anomaly was due to surface contamination of the vapor-phase n layers originally used, and that the MBE Be-doping technique is under satisfactory control.

(ii) Gettering

At the time of submission of our initial proposal, it was believed that substantial oxygen contamination of MBE films might be encountered. However, high mobilities of the films shown in this report and DLTS data prove that oxygen is not a major or even detectable impurity in MBE layers grown under readily-attainable ultrahigh vacuum conditions; these studies have therefore not been pursued.

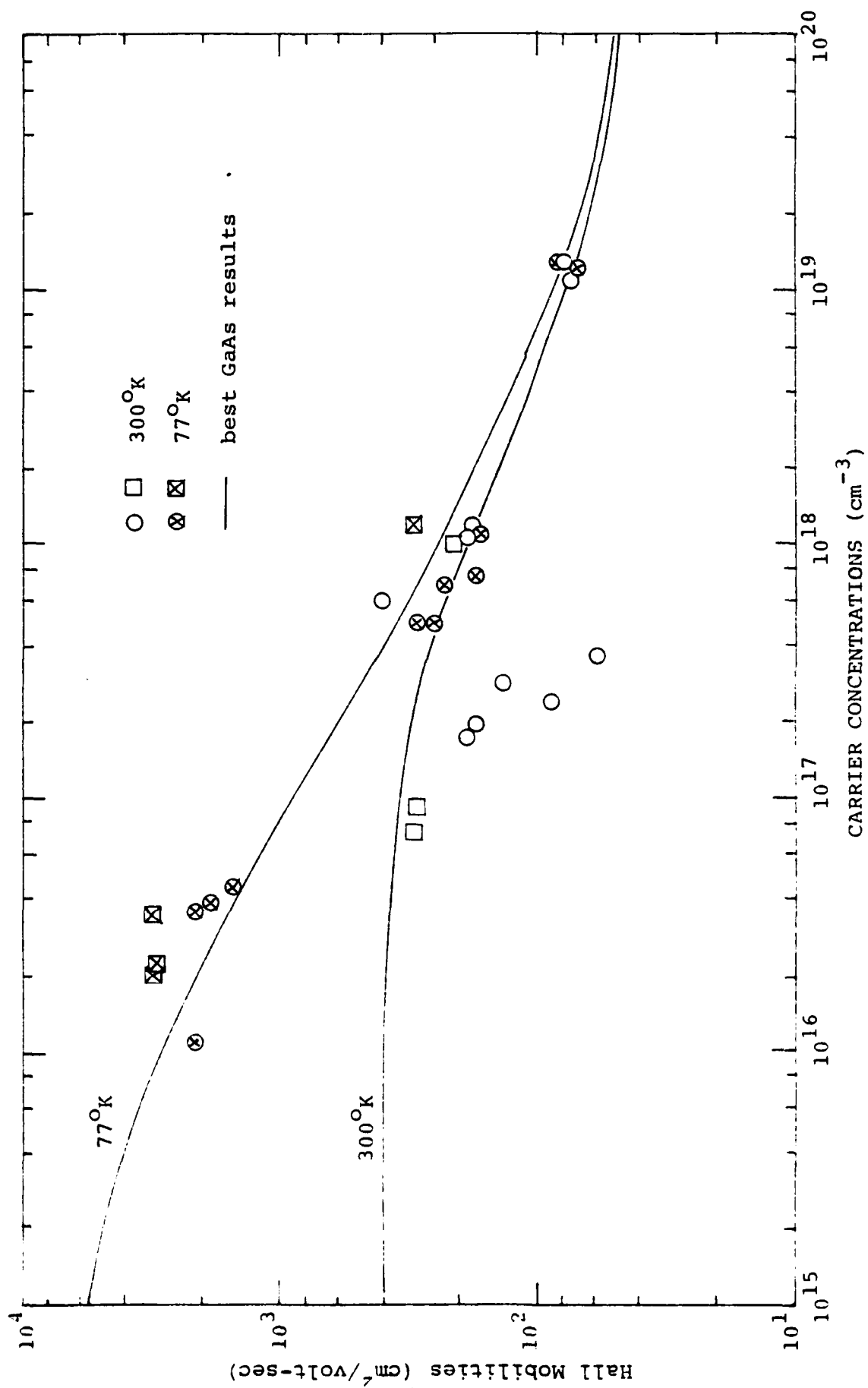


Fig. 13 Room temperature and 77°K Hall mobilities of Be-doped MBE GaAs.

(iii) Background Additives

Inhibition of incorporation of impurities from the background in the MBE by specific additives (e.g., hydrogen) had been reported.¹⁵ However, we have found that hydrogen additives increase the layer mobilities only in the case of rather poor vacuum conditions, and that the mobilities obtained are no better than those resulting when layers are grown under good vacuum in the absence of hydrogen. This investigation was therefore terminated.

IV. CONCLUSIONS

A number of dopants have been used in MBE-GaAs with varying degrees of success -- Sn, Ge, Si, PbSe,¹⁶ PbTe,¹⁶ and SnTe. Each dopant has merits and demerits. Work reported here shows that Si is a near ideal dopant for GaAs device applications. The Si donor is not as heavily compensated as the Ge donor and does not have surface segregation problems like Sn. Also, reproducibility is excellent. We have demonstrated that the "deep levels" associated with Si as a dopant by other workers are not intrinsic, but rather artifacts of effusion cell design. Also, we have shown that higher growth rates can be employed in growing MBE-GaAs without sacrificing the electrical and optical characteristics of the films. This fact should make the MBE technique an economical process for growing microwave and optoelectronic devices. All the experiments on the effects of accelerated growth rates were made on Si-doped films, but higher growth rates could be employed using other dopants. Nevertheless, Si appears to be the best choice because its incorporation is least sensitive to growth conditions, giving the greatest flexibility in determining growth conditions.

One problem in using Si as a donor may be that very high doping concentrations ($>1 \times 10^{19} \text{ cm}^{-3}$) may be difficult to obtain. We have recent evidence that the Si donor starts to be heavily compensated by the Si acceptor at high concentrations and that net donor concentrations above $6 \times 10^{18} \text{ cm}^{-3}$ become difficult to obtain. This makes it desirable to investigate other dopants for degenerate doping of contact layers, for example. It has been demonstrated⁵ that very high doping of GaAs by Ge ($7.4 \times 10^{19} \text{ cm}^{-3}$ free electrons and $3.0 \times 10^{20} \text{ cm}^{-3}$ free holes at 300°K) can be obtained at high As_4/Ga flux ratios (of the order of 10/1). However, reproducible, consistent doping was only obtained up to a plateau of $3 \times 10^{18} \text{ cm}^{-3}$, at which point the material was already appreciably compensated. At still higher doping levels, the materials turned n-type, with a region of instability in between. Mobilities in the

highly-doped regions were of the order of $10 \text{ cm}^2/\text{V-sec}$ for both electrons and holes. As a practical matter, the high As/Ga ratio requires that a As crucible be refilled at more frequent intervals. Also, high As flux tends to degrade surface morphology.

Sn is currently more popular and high doping is possible using it, but SnTe can be an attractive alternative to Sn. Our results show that SnTe doping produced a sharp doping profile change up to the doping concentration of $1 \times 10^{19} \text{ cm}^{-3}$ when used at a substrate temperature of 500-550°C. Also, SnTe-doped films exhibit good mobilities and photoluminescence over a wide doping range of $1 \times 10^{15} \text{ cm}^{-3}$ to $1 \times 10^{19} \text{ cm}^{-3}$. We have found that at a substrate temperature higher than 580°C, Sn and Te segregation does occur, but the segregation is minimal compared to elemental Sn- or Te-doped films. This lesser segregation is probably due to the specific SnTe incorporation mechanism. It appears that SnTe molecules incorporate mostly as Sn and Te pairs instead of independent Sn and Te atoms, and this incorporation mechanism suppresses the surface segregation. We have also found that SnTe incorporation depends on the availability of Ga vacancies.

Our results also showed that the densities of Sn and Te in the SnTe-doped films are comparable, which is to be expected from pair incorporation. The exact nature of the pair incorporation mechanism is not well understood. One thing relatively certain is that SnTe does not incorporate as a molecule. If it does, it should form a deep donor (25 meV - 30 meV), and we have found no evidence of deep donor present in SnTe-doped films. Also, our DLTS results indicate that SnTe doping does not introduce high density deep traps in the film.

REFERENCES

1. A. Y. Cho, J. Vac. Sci. Technol. 16, 275 (1979).
2. P. E. Luscher, W. S. Knodle and Y. G. Chai, Electronics 53, 160 (1980).
3. B. A. Joyce, Surface Sci. 86, 92 (1979).
4. C. E. C. Wood and B. A. Joyce, J. Appl. Phys. 49, 4584 (1978).
5. G. M. Metze, R. A. Stall, C. E. C. Wood and L. F. Eastman, Appl. Phys. Lett. 37, 165 (1980).
6. A. Y. Cho, J. Appl. Phys. 46, 1733 (1975).
7. T. Murotani, T. Shimano and S. Mitsui, J. Crys. Growth 45, 302 (1978).
8. A. Y. Cho and I. Hayashi, Met. Trans., 2, 777 (1971).
9. T. Shimano, T. Murotani, M. Nakatani, M. Otsubo and S. Mitsui, Surface Sci. 86, 126 (1979).
10. D. M. Collins, Appl. Phys. Lett. 35, 67 (1979).
11. A. Y. Cho and J. R. Arthur, Progress in Solid State Chem. 10, 157 (1975).
12. R. Colin and J. Prowart, Trans. Faraday Soc. 60, 673 (1964).
13. A. C. Gossard, P. M. Petroff, W. Wiegmann, R. Dingle and A. Savage, Appl. Phys. Lett. 29, 323 (1976).
14. C. J. Smithells (Ed.), Metals Reference Book, 5th Ed. (Butterworths, London, 1976).

15. A. R. Calawa, Appl. Phys. Lett. 33, 1020 (1978).
16. C. E. C. Wood, Appl. Phys. Lett. 33, 770 (1978).

PUBLICATIONS

1. Y. G. Chai, "Effects of Accelerated Growth Rate (1-5 $\mu\text{m/hr}$) for MBE GaAs Using Si as a Dopant," J. Appl. Phys. Lett. 37, 379 (1980).
2. Y. G. Chai, R. Chow, D. M. Collins and J. N. Miller, "Dopant Incorporation of SnTe in MBE GaAs", to be submitted to J. Appl. Phys.

Effect of accelerated growth rate (1–5 $\mu\text{m/h}$) on molecular beam epitaxial GaAs using Si as a dopant

Young G. Chai

Corporate Solid State Laboratory, Varian Associates, Inc., Palo Alto, California 94303

(Received 24 April 1980; accepted for publication 16 June 1980)

The slow growth rate of molecular beam epitaxy (MBE) allows close to monolayer control of the film thickness. However, if the growth rate can be increased without significant loss of material quality or control, MBE may also become an economical way to grow epitaxial layers for optoelectronic and microwave devices. In this work, Si was studied as an n -type dopant at various growth rates. Hall mobilities of 60 036 $\text{cm}^2/\text{V sec}$ at 77 K and 8839 $\text{cm}^2/\text{V sec}$ at room temperature were achieved using a 1- $\mu\text{m/h}$ growth rate. Higher mobilities were obtained at higher growth rates. Photoluminescence spectra of Si-doped films were dominated by near-band-edge emission. The growth rate of MBE GaAs can be increased at least up to 5 $\mu\text{m/h}$ without change in electrical and optical characteristics of films.

PACS numbers: 68.55. + b, 78.55.Ds

Molecular beam epitaxy (MBE) is a fast-emerging technology for epitaxial growth showing signs of becoming a practical crystal growth technique for optoelectronic and microwave devices. One of the main features of MBE is its precise layer thickness control. It has been demonstrated that a superlattice structure, consisting of thousands of alternating monolayers of GaAs and AlAs, can be grown by MBE.¹ Naturally, MBE has been successful for devices that require growth of thin layers in the structure, such as lasers, mixers, IMPATT diodes, and low-noise field-effect transistors. (For a review, see Ref. 2.) Presently 1 $\mu\text{m/h}$ is a typical MBE growth rate for GaAs. If higher growth rates can be employed without sacrificing device performance and yield, MBE may become economical for optoelectronic and microwave devices. This letter investigates this possibility by studying the electrical and optical characteristics of Si-doped GaAs layers grown at different rates.

In order to investigate higher-growth-rate effects, it is desirable to find a dopant which is not sensitive to the change of growth conditions. Many elements and compounds have been used as n -type dopants, i.e., Sn,³ SnTe,⁴ Ge,⁵ PbS,⁶ PbSe,⁷ and Si.⁷ Among these, Si appears to be least sensitive to growth conditions. The Si incorporation rate is indepen-

dent of substrate temperature from 500 to 600 °C and is insensitive to As₄/Ga ratio change. Also, doping to $2.5 \times 10^{18} \text{ cm}^{-3}$ is possible.^{7,8} One of the reasons that Si is not widely used in MBE may be the concern over the relatively high operating temperature required for the Si furnace (> 1200 °C). Out-gassing of undesirable impurities from heating elements may result in film contamination. However, no such effects were clearly found during the course of this work.

All the epitaxial growths were performed in a Varian MBE-360 molecular beam epitaxy system. A detailed system description can be found elsewhere.⁹ The molecular beam sources were standard Varian MBE furnaces containing charges of Ga (7N, Eagle-Pitcher), As (6N, Canyonlands 21st Century Corp.), and Si (10^{13} cm^{-3} phosphorus doped, Dow Corning). All the charges were contained in pyrolytic boron nitride (PBN) crucibles. The substrate material was (100) oriented Cr-doped GaAs grown in this laboratory by the liquid encapsulation Czochralski process. The substrates were chemomechanically polished in standard sodium hypochlorite solution. Immediately before loading, the substrates were degassed in TCE, acetone, and methanol and etched in stagnant 4:1:1 ($\text{H}_2\text{SO}_4:\text{H}_2\text{O}_2:\text{H}_2\text{O}$) solution for one

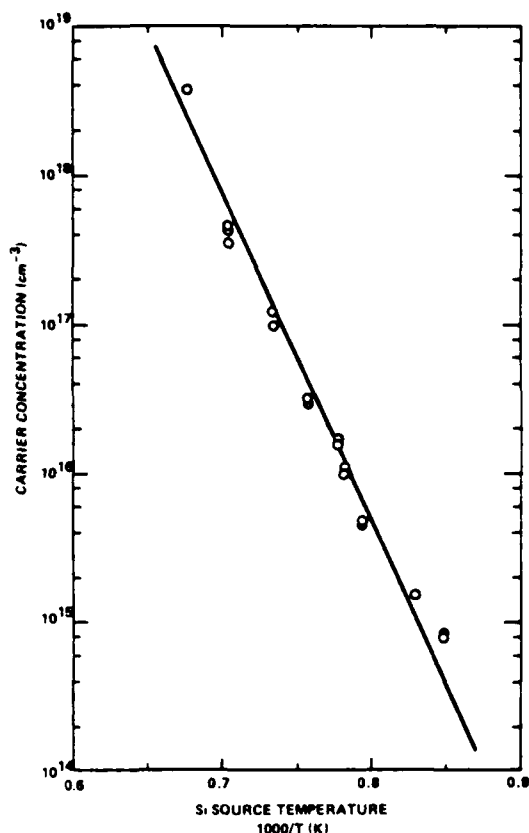


FIG. 1. Carrier concentration measured by the Van der Pauw technique as a function of reciprocal temperature of the Si furnace.

minute. Indium was used to bond the substrate to a molybdenum heater block. The substrate was heat cleaned in the growth chamber for six minutes at 611 °C with the As furnace open. All GaAs films reported here were grown at a substrate temperature of 581 °C with $J_{As}/J_{Ga} = 0.75-1.00$, where J_{As}/J_{Ga} are the arsenic and gallium flux densities. The Si furnace temperature ranged from 850 to 1200 °C. Typical background pressure during growth was 5×10^{-7} Torr for $1 \mu/h$ and increased linearly with growth rate. The Hall mobilities were measured by the Van der Pauw technique on 2.5–3.0- μ -thick layers grown directly on Cr-doped substrates, without a buffer. The magnetic field was 1.2 kG. The epitaxial layer thickness determined by cleave and stain measurement was used for calculation of carrier concentration. Photoluminescence (PL) measurements were made at 77 K with a 1-W argon laser and cooled S-1 photomultiplier.

Figure 1 shows the measured carrier concentration as a function of reciprocal temperature of the Si furnace. The solid line in the figure represents the vapor pressure of Si vs $1/T$,¹⁰ with the position of the ordinate scale adjusted to coincide with the experimental data points. The experimental points were obtained on films grown at $1 \mu/h$. The fact that the slope of the vapor pressure curve agrees well with the experimental points suggests that, over the concentration range studied, the Si doping level is proportional to the Si arrival rate. The doping concentration at higher growth rates can be predicted from this curve within 20% error.

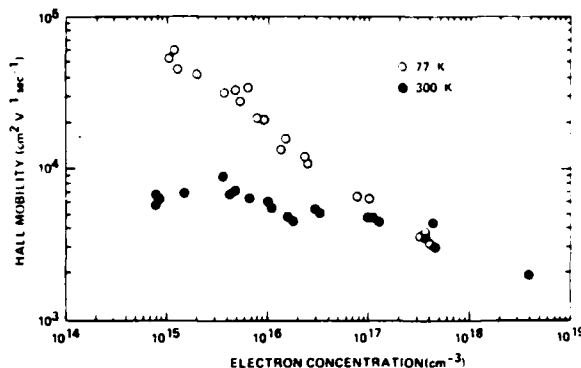


FIG. 2. Room-temperature and 77-K Hall mobilities of Si-doped films grown at $1 \mu/h$.

Figure 2 shows the Hall mobilities versus doping concentration for Si-doped layers grown at $1.0 \mu/h$. The results compare favorably with those reported in the literature for MBE GaAs. The highest room-temperature mobility was $8839 \text{ cm}^2/\text{V sec}$ at $3.6 \times 10^{15} \text{ cm}^{-3}$, and the highest 77-K mobility was $60\,036 \text{ cm}^2/\text{V sec}$ at $1.2 \times 10^{15} \text{ cm}^{-3}$.

Films grown at higher growth rates were doped at $10^{15}-10^{16} \text{ cm}^{-3}$, so that possible change in the mobilities could be seen more easily. Since many different growth rates were tried, most are grouped together and presented in Fig. 3. As shown in the figure, there is about 50% spread in mobility at a given carrier concentration. The same degree of variation is observed even for films grown at the same rate of $1 \mu/h$. This variation is probably a result of compounding measurement errors and differences in substrate quality. The highest 77-K mobility achieved was $75\,085 \text{ cm}^2/\text{V sec}$ at $2.2 \times 10^{15} \text{ cm}^{-3}$ for the film grown at $1.8 \mu/h$. From these results, it can be concluded that the mobilities at higher growth rates are comparable to or higher than those at $1 \mu/h$.

The accelerated growth rate did not produce any significant changes in the 77-K PL spectra. Spectra for wafers grown at 1 and $5 \mu/h$ are shown in Figs. 4(a) and 4(b). The

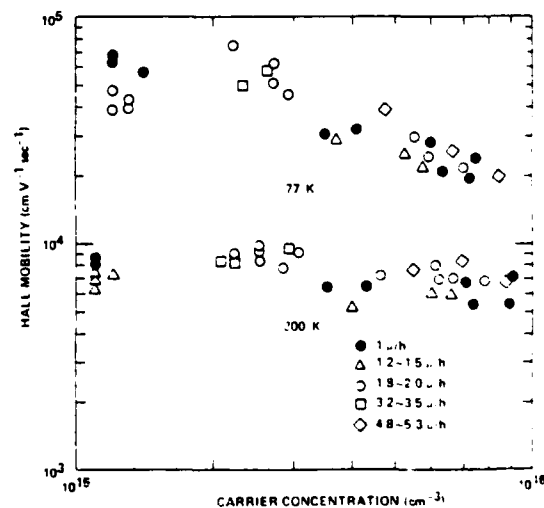


FIG. 3. Room-temperature and 77-K Hall mobilities of films grown at 1–5 μ/h growth rates.

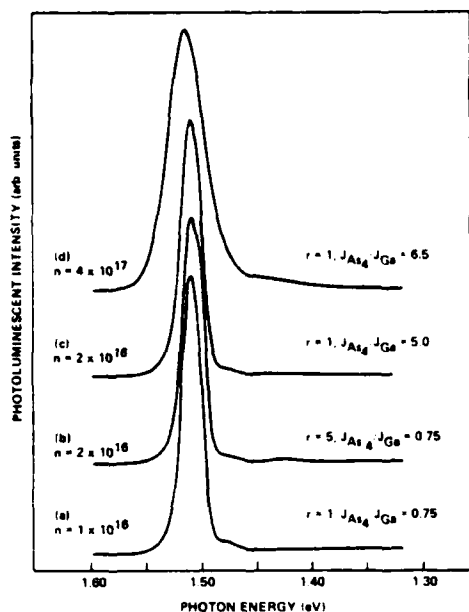


FIG. 4. PL spectrum for films grown under different conditions: (a) normal conditions, (b) five times higher rate, (c) normal growth rate but with a six times higher J_{As_4}/J_{Ga} ratio, (d) highly doped GaAs grown with eight times higher J_{As_4}/J_{Ga} ratio (r designates the growth rate).

donor-to-valence-band transition at 1.507 eV dominates in both spectra. The donor-to-acceptor transition at 1.477 eV is also observed. However, the energy peaks observed by others in Si-doped MBE GaAs at 1.44 eV,⁸ or about 1 eV below the edge emission peak¹¹ are very weak or absent. These peaks have been associated with an impurity-Ga vacancy complex. The small J_{As_4}/J_{Ga} ratio used for the growth of Fig. 4(a) and 4(b) wafers would have decreased the number of Ga vacancies. In order to check this hypothesis, a third wafer

was grown with an As flux five times higher than normal. PL from this wafer is shown in Fig. 4(c). Again, the lower-energy peak is small. Finally, a highly doped ($4 \times 10^{17} \text{ cm}^{-3}$) film was grown under very high As flux density. As shown in Fig. 4(d), there is no significant increase in the lower-energy peak. It appears that the lower-energy peak is neither inherently connected with Si doping nor directly associated with availability of Ga vacancies, but may be associated with general cleanliness of the growth system or substrate qualities.

Even though there is little difference in electrical and optical characteristics of films grown at different growth rates, a difference in surface morphology is sometimes observed. The layer grown at $1 \mu/\text{h}$ has a very smooth surface, as shown in Fig. 5(a). However, as the growth rate is raised, the grown surface sometimes reveals spurious growths, as shown in Fig. 5(b). This spurious growth is also observed for films grown at $1 \mu/\text{h}$ when the As flux is high. This problem seems to be associated with the Ga spitting that Wood *et al.* described in their recent work.¹²

In conclusion, Si-doped films exhibit high mobilities and good PL characteristics. Higher growth rates yield comparable or better 77-K mobilities and do not significantly affect PL characteristics. High Ga evaporation rate and high As pressure sometimes result in spurious growths on the surface. However, this problem can be minimized by filling the Ga crucible full and avoiding excessive use of As flux during growth.

The author wishes to thank the Varian Vacuum Division, especially P. E. Luscher, for providing the Varian MBE-360 used for the experiment. Careful manuscript reading and suggestions by R. L. Bell and J. S. Escher are appreciated. Also, thanks are due to C. E. C. Wood for a preprint of Ref. 12. Special thanks are due to M. Pustorino for her technical assistance. This work was supported by the Air Force Office of Scientific Research, under Contract No. F 49620-80-C-0011.

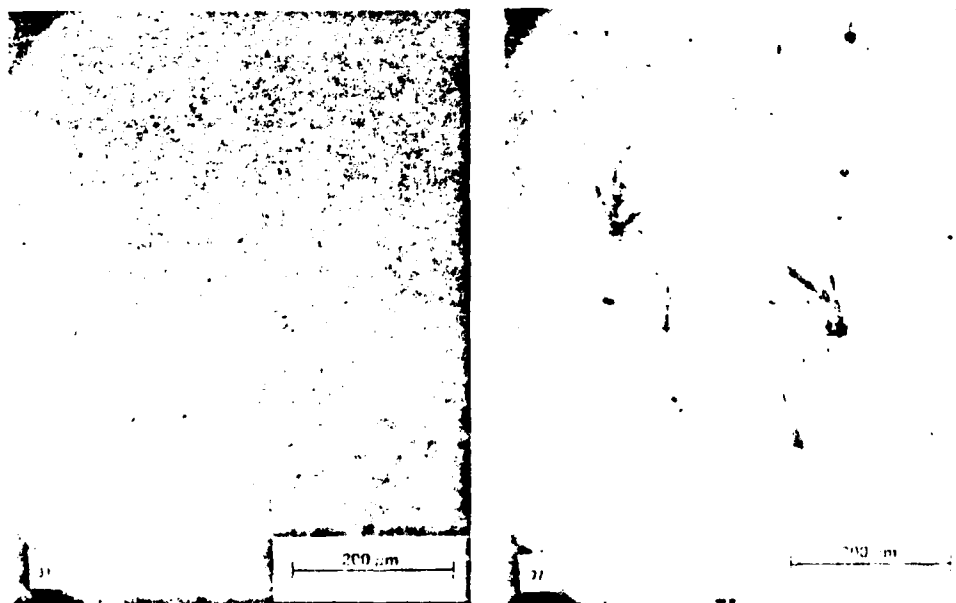


FIG. 5. As-grown surface morphology of MBE GaAs. (a) smooth surface grown under normal conditions, (b) spurious growth on the surface

- ¹A. C. Gossard, P. M. Petroff, W. Wiegmann, R. Dingle, and A. Savage, *Appl. Phys. Lett.* **29**, 323 (1976).
- ²A. Y. Cho, *J. Vac. Sci. Technol.* **16**, 275 (1979).
- ³C. E. C. Wood and B. A. Joyce, *J. Appl. Phys.* **49**, 4854 (1978).
- ⁴D. M. Collins, *Appl. Phys. Lett.* **35**, 67 (1979).
- ⁵C. E. C. Wood, J. Woodcock, and J. J. Harris, in *Proceedings of the Biannual Conference on Gas and Related Compounds, St. Louis, 1978* (Institute of Physics, London, 1979).
- ⁶C. E. C. Wood, *Appl. Phys. Lett.* **33**, 770 (1978).
- ⁷T. Murotani, T. Shimanoe, and S. Mitsui, *J. Cryst. Growth* **45**, 302 (1978).
- ⁸T. Shimanoe, T. Murotani, M. Nakatani, M. Otsubo, and S. Mitsui, *Surf. Sci.* **86**, 126 (1979).
- ⁹P. E. Luscher, *Solid State Technol.* **20**, 43 (1977).
- ¹⁰*Metals Reference Book*, 5th ed., edited by C. J. Smithells (Butterworths, London, 1976).
- ¹¹A. Y. Cho and I. Hayashi, *Metall. Trans.* **2**, 777 (1971).
- ¹²C. E. C. Wood, L. Rathbun, and H. Ohno, *J. Cryst. Growth* (to be published).

DATE
ILME